

# CRAMER-RAO BOUNDS FOR RANGE AND MOTION PARAMETER ESTIMATIONS USING DUAL FREQUENCY RADARS

*Pawan Setlur, Moeness Amin, and Fauzia Ahmad*  
Radar Imaging Lab, Center for Advanced Communications  
Villanova University, Villanova, PA 19085, USA

## ABSTRACT

In this paper, statistical bounds on dual-frequency range estimations are provided. Single frequency (Doppler) radars cannot be used in range estimation due to their range ambiguities. An additional frequency can be used to increase the maximum unambiguous range to accepted values for indoor range estimation of moving targets. The dual-frequency approach offers the benefit of reduced complexity, fast computation time, and real time target tracking. Indoor inanimate objects such as fans, vibrating machineries, and clock pendulums exhibit simple harmonic motions, whereas animate translation movements are typically linear. We provide Cramer-Rao bounds for the parameters defining both types of motions and show their dependency on the observation period and partial knowledge of motion and noise parameters.

**Index Terms**—CW radar, Doppler radar, Random Noise.

## 1. INTRODUCTION

Urban sensing is an emerging area of research and development which requires rapid motion identification and builds on advances in high resolution imaging [1, 2]. Acoustics, ultrasound, and RF technologies can be used to provide target detection, location, and classification. Common constraints are imposed on all three technologies, namely, cost, weight, reliability, and user- friendly interface.

In this paper, we focus on Doppler radars for both target motion detection and ranging. Doppler radars meet operation constraints and can function well in highly cluttered indoor scenes. The bounds on target locations imposed by the room and building dimensions allow range estimation of moving targets using only two different frequencies. The dual-frequency approach has long been proposed for general radar applications [3, 4], but is likely to emerge as one of the leading approaches in urban sensing.

In this paper, we develop Cramer Rao bounds for indoor moving target parameters using the dual frequency approach. We consider targets with linear and simple harmonic motions (SHM). For both cases, in addition to motion speed and harmonic frequency, the CRB on the

range estimate is also provided.

## 2. RANGE AMBIGUITY

Consider a CW radar having a single carrier frequency  $f$ . The phase of the returns is range dependent, and is expressed as

$$\phi(n) = \frac{4\pi f}{c} R(n), n = 0, 1, 2, \dots, N-1 \quad (1)$$

where  $R(n)$  is the range of the target for sample  $n$ . Since the phase is modulo  $2\pi$ , then the maximum unambiguous range, denoted by  $R_u$ , is expressed as

$$R_u = \frac{c}{2f} \quad (2)$$

Typical radar applications involve large carrier frequencies in the MHz-GHz range; hence, the respective maximum unambiguous ranges are in a few centimeters, which are unacceptable values for target location estimation. However, consider a radar system employing two distinct carrier frequencies  $f_1$ , and  $f_2$ . The phase of the returns are given by,

$$\phi_1(n) = \frac{4\pi f_1}{c} R(n), \phi_2(n) = \frac{4\pi f_2}{c} R(n) \quad (3)$$

Consider the difference in the unwrapped phase, expressed as,

$$\phi_2(n) - \phi_1(n) = \frac{4\pi(f_2 - f_1)}{c} R(n) \quad (4)$$

The maximum unambiguous range is obtained by letting the LHS of eq. (4) equal to  $2\pi$ .

$$R_u = \frac{c}{2(f_2 - f_1)} \quad (5)$$

From eq. (5), two frequencies of 1 GHz and 1.01 GHz can increase the maximum unambiguous range for 15cm to 15m, which can be sufficient for target location in rooms and small buildings. It is noted that closer values of the two employed frequencies can lead to higher unambiguous range. However, coherent phase estimation can be compromised if the frequency difference is too small to overcome noise effects, large Doppler and micro-Doppler frequencies, and frequency drifts in down conversions.

---

This work was supported by DARPA under grant no. MDA972-02-1-0022. The content of the information does not necessarily reflect the position or the policy of the Government, and no official endorsement should be inferred.

### 3. MODEL

Consider a CW dual frequency radar employing two known carrier frequencies,  $f_1$  and  $f_2$ . The returns are range dependent and expressed as,

$$x_1(n) = \rho \exp\left(j \frac{4\pi f_1 R(n)}{c}\right) + v_1(n) = s_1(n) + v_1(n) \quad (8)$$

$$x_2(n) = \rho \exp\left(j \frac{4\pi f_2 R(n)}{c}\right) + v_2(n) = s_2(n) + v_2(n) \quad (9)$$

$$\{n | n \in \mathbb{Z}^+, n = 0, 1, 2, 3, \dots, N-1\}$$

where,  $R(n)$  is the range of target, which is a function of time,  $c$  is the speed of light in free space and  $\rho$  is the return signal amplitude.  $\mathbb{Z}^+$  is defined as the domain of positive integers. The noise over the observation period,  $N$ , is AWGN and uncorrelated, i.e.,

$$v_1(n) \sim \mathcal{N}(0, \sigma_1^2), v_2(n) \sim \mathcal{N}(0, \sigma_2^2), E\{v_1(n)v_2(n)\} = 0$$

where  $\sigma_1^2$  and  $\sigma_2^2$  represent the noise variance for the two radars, respectively. For linear motion, the target is moving with a constant velocity,  $v$ , and the time-dependent range is  $R(n) = R_o + vn$  (10)

The target range for micro-Doppler (SHM) motion at sample  $n$ , is parameterized as [5]

$$R(n) = R_o + d \cos(\omega_o n - \phi_o) \quad (11)$$

where  $d$ ,  $\omega_o$ , and  $\phi_o$  are the maximum displacement, micro-Doppler frequency and phase, respectively. In eqs. (10)-(11), the parameter,  $R_o$ , is the initial target range.

### 4. CRAMER RAO BOUNDS

The received data from the radar forms long vectors,

$$\mathbf{x} = [x_1(0), x_1(1), x_1(2), \dots, x_1(N), x_2(0), x_2(1), \dots, x_2(N)]^T \quad (12)$$

$$= [\mathbf{x}_1 \quad \mathbf{x}_2]^T$$

$$\mathbf{s} = [s_1(0), s_1(1), s_1(2), \dots, s_1(N), s_2(0), s_2(1), \dots, s_2(N)]^T \quad (13)$$

$$= [\mathbf{s}_1 \quad \mathbf{s}_2]^T$$

$$\mathbf{v} = [v_1(0), v_1(1), v_1(2), \dots, v_1(N), v_2(0), v_2(1), \dots, v_2(N)]^T \quad (14)$$

$$= [\mathbf{v}_1 \quad \mathbf{v}_2]^T$$

The mean and covariance matrix of  $\mathbf{x}$  are given by

$$E\{\mathbf{x}\} = \boldsymbol{\mu} = [\mathbf{s}_1 \quad \mathbf{s}_2]^T \quad (15)$$

$$E\{(\mathbf{x} - \boldsymbol{\mu})(\mathbf{x} - \boldsymbol{\mu})^H\} = \mathbf{C} = \begin{bmatrix} \sigma_1^2 \mathbf{I} & \mathbf{0}_N \\ \mathbf{0}_N & \sigma_2^2 \mathbf{I} \end{bmatrix} \quad (16)$$

Let the parameter vector be  $\boldsymbol{\theta} = [\theta_1, \theta_2, \theta_3, \dots, \theta_k]^T$ . The Fisher information elements for independent identically distributed (i.i.d) complex Gaussian samples is given by [6]

$$[\mathbf{F}(\boldsymbol{\theta})]_{pq} = \text{Tr} \left[ \mathbf{C}^{-1} \frac{\partial \mathbf{C}}{\partial \theta_p} \mathbf{C}^{-1} \frac{\partial \mathbf{C}}{\partial \theta_q} \right] \quad (17)$$

$$+ 2 \text{Re} \left\{ \frac{\partial \mathbf{s}^H(\boldsymbol{\theta})}{\partial \theta_p} \mathbf{C}^{-1} \frac{\partial \mathbf{s}(\boldsymbol{\theta})}{\partial \theta_q} \right\}, (p, q) = 1, 2, \dots, k$$

where  $\text{Re}\{\cdot\}$  denotes the real part,  $\mathbf{F}(\boldsymbol{\theta})$  is the fisher information matrix (FIM), and  $\text{Tr}(\cdot)$  is the trace operator. The Cramer Rao bounds (CRB's) are the inverse of the fisher information, and appear on the diagonal of the inverted FIM.

$$\text{CRB}(\theta_p) = [\mathbf{F}^{-1}(\boldsymbol{\theta})]_{pp} \leq \text{var}(\hat{\theta}_p) \quad (18)$$

Due to the diagonal assumption of the covariance matrix  $\mathbf{C}$ , the first term in eq. (17) is zero. Before we proceed with the derivations, we introduce certain parameters to make the CRB analysis more generic.

$$\gamma := f_2 / f_1, \quad \psi := \frac{\sigma_1^2}{\sigma_2^2} \quad \text{and} \quad \text{SNR}_1 := \frac{\rho^2}{\sigma_1^2} \quad (19)$$

We evaluate the CRB's as functions of the parameters defined in eq. (19) and the number of data samples,  $N$ .

#### 4.1. Constant Doppler

In this case the parameter vector is  $\boldsymbol{\theta} = [R_o \quad v]^T$ . Substituting eq. (10) for Doppler motion in eqs. (8)-(9), we obtain the signal returns. Now, using the signal returns for constant Doppler in eq. (17), we obtain the FIM. It can be readily shown that for a single Doppler frequency radar, employing carrier  $f_1$ , the FIM,  $\mathbf{F}_{f_1}$ , and its inverse, is

$$\mathbf{F}_{f_1} = \frac{32\pi^2 \text{SNR}_1 f_1^2}{c^2} \begin{bmatrix} N & \frac{N(N-1)}{2} \\ \frac{N(N-1)}{2} & \frac{N(N-1)(2N-1)}{6} \end{bmatrix} \quad (20)$$

$$\mathbf{F}_{f_1}^{-1} = \frac{\lambda_1^2}{\text{KSNR}_1} \begin{bmatrix} \frac{2(2N-1)}{N(N+1)} & \frac{-6}{N(N+1)} \\ \frac{-6}{N(N+1)} & \frac{12}{N(N^2-1)} \end{bmatrix} \quad (21)$$

where  $\lambda_1 = c/f_1$ , and  $\text{K} = 32\pi^2$  a constant. However, for the proposed dual frequency radar the FIM is given by

$$\mathbf{F} = \frac{32\pi^2 \text{SNR}_1 f_1^2}{c^2} (1 + \gamma^2 \psi) \begin{bmatrix} N & \frac{N(N-1)}{2} \\ \frac{N(N-1)}{2} & \frac{N(N-1)(2N-1)}{6} \end{bmatrix} \quad (22)$$

$$\mathbf{F}^{-1} = \frac{\lambda_1^2}{\text{KSNR}_1 (1 + \gamma^2 \psi)} \begin{bmatrix} \frac{2(2N-1)}{N(N+1)} & \frac{-6}{N(N+1)} \\ \frac{-6}{N(N+1)} & \frac{12}{N(N^2-1)} \end{bmatrix} \quad (23)$$

It is clear from eq. (20) and eq. (22) that the Fisher information for the proposed dual frequency scheme can be written as,

$$\mathbf{F} = \mathbf{F}_{f_1} + \mathbf{F}_{f_2} \quad (24)$$

The diagonal elements in eq. (23) represent the CRB's for the target range and velocity under constant Doppler motion. It is evident from the multiplicative factor in eqs. (21) and (23) that the CRB's for both the initial range and velocity for the dual frequency case consistently assume smaller values as compared to the single frequency operation.

## 4.2 Micro-Doppler

In this case, the parameter vector is  $\boldsymbol{\theta} = [R_o \ d \ \omega_o \ \phi_o]^T$ . Substituting eq. (11) for micro-Doppler motion in eqs. (8)-(9), we obtain the signal returns, which are in turn used in eq. (17) to compute the FIM.

$$\mathbf{F} = \begin{bmatrix} F_{R_o R_o} & F_{R_o d} & F_{R_o \omega_o} & F_{R_o \phi_o} \\ F_{d R_o} & F_{dd} & F_{d \omega_o} & F_{d \phi_o} \\ F_{\omega_o R_o} & F_{\omega_o d} & F_{\omega_o \omega_o} & F_{\omega_o \phi_o} \\ F_{\phi_o R_o} & F_{\phi_o d} & F_{\phi_o \omega_o} & F_{\phi_o \phi_o} \end{bmatrix} \quad (25)$$

$$= \begin{bmatrix} \mathbf{F}_1 & \mathbf{F}_3 \\ \mathbf{F}_3^T & \mathbf{F}_2 \end{bmatrix}$$

In the above equation, it is noted that  $F_{ij} = F_{ji}, \forall i = j = 1, 2, 3, 4$ . Hence, it is sufficient to derive the upper triangular elements only. We define  $\frac{KSNR_1}{\lambda_1^2} (1 + \gamma^2 \psi) = \varepsilon$ , and proceed with the derivation.

$$F_{R_o R_o} = \varepsilon N \quad (26)$$

$$F_{R_o d} = \varepsilon \frac{\cos\left(\omega_o \frac{N-1}{2} - \phi_o\right) \sin\left(\frac{\omega_o N}{2}\right)}{\sin\left(\frac{\omega_o}{2}\right)} \quad (27)$$

$$F_{R_o \omega_o} = \frac{\varepsilon d}{4 \sin^2\left(\frac{\omega_o}{2}\right)} \left( (2N-1) \sin\left(\frac{\omega_o}{2}\right) \cos\left(\omega_o \frac{2N-1}{2} - \phi_o\right) - \cos\left(\omega_o \frac{N-1}{2} - \phi_o\right) \sin\left(\omega_o \frac{2N-1}{2} - \phi_o\right) - \sin(\phi_o) \right) \quad (28)$$

$$F_{R_o \phi_o} = \varepsilon d \left( \frac{\sin\left(\omega_o \frac{N-1}{2} - \phi_o\right) \sin\left(\frac{\omega_o N}{2}\right)}{\sin\left(\frac{\omega_o}{2}\right)} \right) \quad (29)$$

$$F_{dd} = \frac{\varepsilon}{2} \left( \frac{\cos(\omega_o(N-1) - 2\phi_o) \sin(\omega_o N)}{\sin(\omega_o)} + N \right) \quad (30)$$

$$F_{d \omega_o} = \frac{\varepsilon d}{8 \sin^2(\omega_o)} \left( (2N-1) \sin(\omega_o) \cos(\omega_o(2N-1) - 2\phi_o) - \cos(\omega_o) \sin(\omega_o(2N-1) - 2\phi_o) - \sin(2\phi_o) \right) \quad (31)$$

$$F_{d \phi_o} = \frac{\varepsilon d}{2} \left( \frac{\sin(\omega_o(N-1) - 2\phi_o) \sin(\omega_o N)}{\sin(\omega_o)} \right) \quad (32)$$

$$F_{\omega_o \omega_o} = \frac{\varepsilon d^2}{2} \left( \frac{N(N-1)(2N-1)}{6} + \frac{1}{8 \sin^3(\omega_o)} \begin{bmatrix} 2 \cos^2(\omega_o) \sin(\omega_o(2N-1) - 2\phi_o) \\ + 2 \cos(\omega_o) \sin(2\phi_o) \\ - \left( (2N-1) \sin(2\omega_o) \right) \\ \times \cos(\omega_o(2N-1) - 2\phi_o) \\ - \left( 4N(N-1) \sin^2(\omega_o) \right) \\ \times \sin(\omega_o(2N-1) - 2\phi_o) \end{bmatrix} \right) \quad (33)$$

$$F_{\omega_o \phi_o} = \frac{\varepsilon d^2}{2} \left( \frac{1}{4 \sin^2(\omega_o)} \begin{bmatrix} \left( (2N-1) \sin(\omega_o) \right) \\ \times \sin(\omega_o(2N-1) - 2\phi_o) \\ + \cos(\omega_o) \cos(\omega_o(2N-1) - 2\phi_o) \\ - \cos(2\phi_o) \end{bmatrix} - \frac{N(N-1)}{2} \right) \quad (34)$$

$$F_{\phi_o \phi_o} = \frac{\varepsilon d^2}{2} \left( N - \frac{\cos(\omega_o(N-1) - 2\phi_o) \sin(\omega_o N)}{\sin(\omega_o)} \right) \quad (35)$$

To evaluate the CRB's we employ the partitioned matrix inversion lemma, i.e.

$$\mathbf{F}^{-1} = \begin{bmatrix} \left( \mathbf{F}_1 - \mathbf{F}_3 \mathbf{F}_2^{-1} \mathbf{F}_3^T \right)^{-1} & - \left( \mathbf{F}_1 - \mathbf{F}_3 \mathbf{F}_2^{-1} \mathbf{F}_3^T \right)^{-1} \mathbf{F}_3 \mathbf{F}_2^{-1} \\ - \left( \mathbf{F}_2 - \mathbf{F}_3^T \mathbf{F}_1^{-1} \mathbf{F}_3 \right)^{-1} \mathbf{F}_3^T \mathbf{F}_1^{-1} & \left( \mathbf{F}_2 - \mathbf{F}_3^T \mathbf{F}_1^{-1} \mathbf{F}_3 \right)^{-1} \end{bmatrix} \quad (36)$$

Due to intractable expressions involved in the Fisher information elements, we numerically obtain the CRB's for Micro-Doppler in the subsequent section.

## 5. SIMULATIONS

In this section, we evaluate the CRB's for both linear and simple harmonic motions with respect to the data length  $N$ . Fig. 1 shows the  $CRB(v)$  vs.  $N$  for different values of the parameter  $\psi$ . The higher of the two SNR's, corresponding to  $f_1$  and  $f_2$ , is chosen to be 20dB. The corresponding

CRB for a single frequency radar, employing carrier  $f_1$  with an SNR of 20dB, is also provided for comparison. We observe that the CRB for the dual frequency operation is the lowest for  $\psi = 1$ , i.e.  $SNR_1 = SNR_2 = 20\text{dB}$ . For other values of  $\psi$ , the dual-frequency CRB approaches the CRB for single frequency radar, operating at the frequency corresponding to the higher of  $SNR_1$  and  $SNR_2$ . We observe the same trend in Fig. 2, which shows the  $CRB(R_o)$  vs. data length  $N$  for the same parameter values as in Fig. 1. It is obvious from the CRB's that velocity estimates have lower variance than the range estimates. This implies that the data is more sensitive to changes in  $v$  than  $R_o$  [6]. Hence, some design for the order of joint estimation is therefore evidenced from the CRB's.

In Fig. 3, we show the CRB's for micro-Doppler motion vs. the data length  $N$  for  $\psi = 1$  with  $SNR_1 = SNR_2 = 20\text{dB}$ . The  $CRB(\omega_o)$  has the lowest variance amongst all parameters.  $CRB(d)$  and  $CRB(R_o)$  are almost identical in terms of the variance values, whereas  $CRB(\phi_o)$  has the maximum variance amongst all parameters. From our numerical computation, we observed that  $CRB(\omega_o)$  is inversely proportional to  $N^3$ , whereas, the CRB's for the rest of the Micro-Doppler parameters are inversely proportional to  $N$ . Again, this implies that the data is most sensitive to parameter  $\omega_o$  and least sensitive to parameter  $\phi_o$ . Accordingly, the first parameter to be estimated should be  $\omega_o$ .

## 6. CONCLUSIONS

In this paper, we have considered dual frequency radar for range estimation with application to urban sensing. CRBs were derived for range, velocity, and oscillatory frequency of targets encountering linear and simple harmonic motions. It is shown that the dual-frequency approach provides lower bounds as compared to the single frequency counterpart. Numerical computations of the CRB for MD motion, as a function of the observation period reveals that parameter  $\omega_o$  has the lowest bound, whereas the parameter  $\phi_o$  has the highest bound which implies a desirable order for parameter estimation, if they are performed independently.

## 7. REFERENCES

[1] V. Venkatasubramanian and H. Leung, "A novel chaos based high resolution imaging and its applications to through-the-wall imaging," *IEEE Signal Process. Lett.*, Vol. 12, No. 7, pp. 528-531, 2005.  
 [2] G. Wang, M. G. Amin, "Imaging through unknown walls using different standoff distances," *IEEE Trans. Signal Process.*, Vol. 54, No. 10, pp. 4015-4025, 2006.  
 [3] W. D. Boyer, "A duplex, Doppler, phase comparison radar," *IEEE Transactions on Aerospace and Navigational Electronics*, Vol. ANE-10, No. 3, pp. 27-33, 1963.

[4] T. L. Wadley, "Determining relative position by means of transit time of waves," U. S Patent 2907999, 1959.  
 [5] P. Setlur, M. G. Amin, and F. Ahmad, "Indoor imaging of targets undergoing simple harmonic motion using Doppler radars," *Proc. IEEE Symposium on Signal Processing and Information technology*, Dec. 2005.  
 [6] S. M. Kay, *Fundamentals of Statistical Signal Processing- Estimation Theory*, Vol. I, Prentice Hall, 1993.

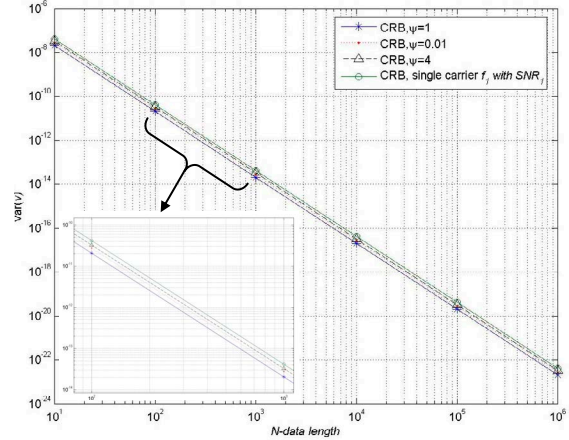


Fig.1. CRB for velocity (constant Doppler motion).

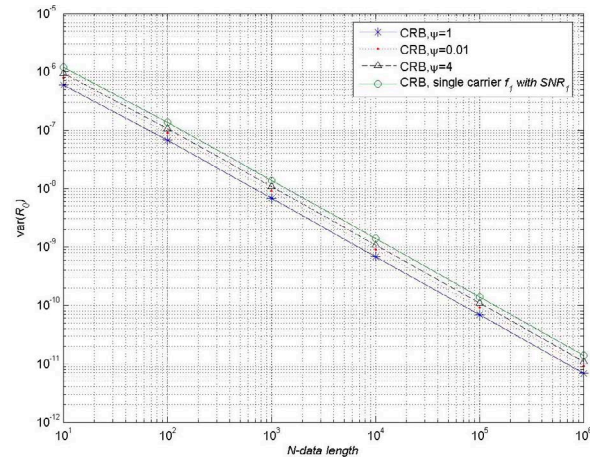


Fig.2. CRB for initial range (constant Doppler motion).

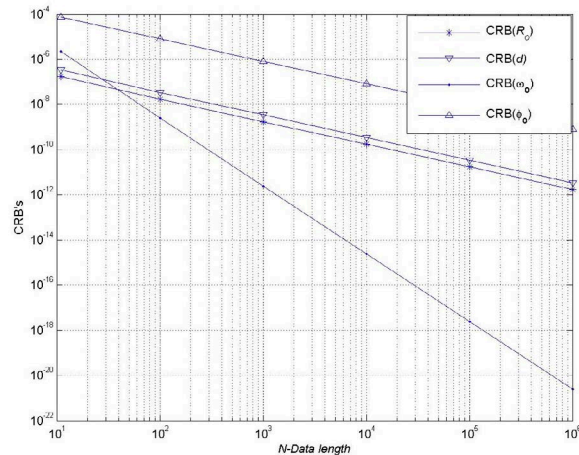


Fig.3. CRB's for Micro-Doppler motion.